https://doi.org/10.3311/PPci.21084

Periodica Polytechnica Civil Engineering, 67(1), pp. 325–335, 2023

Experimental and Numerical Analysis of Impact Strength of Concrete Slabs

Todor Vacev[1*], Andrija Zorić[1], Dušan Grdić[1], Nenad Ristić[1], Zoran Grdić[1], Miloš Milić[1]

[1] Faculty of Civil Engineering, University of Niš, 14 Aleksandra Medvedeva, 18000 Niš, Republic of Serbia
[*] Corresponding author, e-mail: todor.vacev@gaf.ni.ac.rs

Received: 29 August 2022, Accepted: 29 November 2022, Published online: 16 December 2022

Abstract

The topic of this paper is experimental and numerical analysis of the impact strength of unreinforced concrete slabs. Impact strength of concrete is significant in case of some accidental loads during exploitation. Impact strength can be determined experimentally, using Drop-weight test, Charpy test, Projectile impact test, Explosive test, etc. In this research, a numerical model for determining the impact strength of concrete slabs based on Finite element method (FEM) and high-end engineering software has been proposed. Modelling approach to this problem was applying the Explicit dynamics FEM analysis. Thereat, two different existing material models for concrete were enforced: Concrete damage plasticity model – CDP (implemented in ABAQUS/Explicit software), and the Riedel-Hiermaier-Thoma model – RHT (implemented in ANSYS Workbench software). Analysis parameters for both material models, necessary as input data, have been determined through a series of FEM analyses and validated by performed experiments, using drop-weight test. Results of the numerical analyses have been compared with the experimental ones, as well as mutually. Advantages and drawbacks of both material models are highlighted, as well as the reliability of the proposed numerical models. The proposed numerical FE models, confirmed by experiments, can be successfully used for determining impact strength of concrete slabs in further research.

Keywords

concrete slab, impact strength, drop-weight test, FEM, material model

1 Introduction

Impact strength of concrete is defined in literature as toughness of the concrete material under dynamic, i.e., impact load, which is characterized by applying the total proposed load in very short time interval.

Several experimental methods for impact strength determination exist, like Drop-weight test, Charpy test, Projectile impact test, Explosive test, etc. [1].

The most often applied method in practice is the Drop-weight test, because it requires simple test equipment, and is easily adapted to the conditions in situ. The aim of this testing is simulation of some real situations, like impacts of some small objects on roof cover, or falling some weight onto industrial floor surface. The response of concrete under dynamic load is assessed after multiple repeated impacts, whereat the number of drops needed for occurring of the first crack, or total fracture is registered [2].

Strength of the structural elements has been primarily researched under static and dynamic loads, and the need for defining the response of the structural elements under impact load has also been noticed [3]. Thus, impact strength of reinforced concrete (RC) beams [4, 5], as well as RC slabs [5], has been experimentally tested.

Numerical finite element (FE) analysis of RC slabs under drop-weight impact load has been conducted using different material models, such are Riedel-Hiermaier-Thoma – RHT model and Ansys Workbench software package [6], continuous surface cap model and Ansys LS-DYNA software package [7], and concrete damage plasticity model – CDP, available in Abaqus software package [8, 9].

Experimental and numerical research encompassed influence of different parameters on strength of an RC slab under impact load, such are slab thickness, impact location, drop-weight height [7], and reinforcement ratio [7, 10]. The semi-empirical formulae for determining local effects of hard missiles have also been proposed [11].

Recently, the impact strength of post-tensioned slabs [12] and slabs reinforced with bars made of glass and carbon fibers reinforced polymers [13, 14], has been tested.

Cite this article as: Vacev T., Zorić A., Grdić D., Ristić N., Grdić Z., Milić M. "Experimental and Numerical Analysis of Impact Strength of Concrete Slabs", Periodica Polytechnica Civil Engineering, 67(1), pp. 325–335, 2023. https://doi.org/10.3311/PPci.21084

Research is directed mostly on solid slabs without openings, but influence of different opening size and layout in RC slabs on impact strength has been also examined [15].

The experimental results of the impact strength of square concrete slabs under impact load performed by Drop-weight test, which were used to calibrate and validate numerical FE models, are presented in this paper. Two different material models have been used, the CDP model with ABAQUS/ Explicit software, and the RHT model with ANSYS Workbench software.

Mechanical characteristics of concrete used for the numerical models have been determined by appropriate experimental testing of the hardened concrete.

2 Experimental research

As a first stage, examinations of the characteristics of the hardened concrete have been conducted, and after that, examinations of the impact strength of a concrete slab using drop-weight test. Description of both stages is given in detail in the further text.

2.1 Experimental testing of the characteristics of the hardened concrete

Concrete for specimens has been made with 400 kg ordinary Portland cement CEM I 52.5R and 1800 kg three-fraction river aggregate from South Morava River. The shares of individual fractions of aggregate in the mixture were: fraction 0/4 mm (43%), fraction 4/8 mm (23%), and fraction 8/16 mm (34%). The water/binder ratio (w/b) was 0.438. Superplasticizer based on polycarboxylate has been added to the concrete mixture, dosed at 2.40 kg/m^3. Making and curing of concrete specimens for experimental testing has been carried out in accordance with the EN 12390-2 [16]. All physical and mechanical characteristics of the hardened concrete have been examined at concrete age of 90 days.

For the hardened concrete, the following characteristics have been examined: density of the hardened concrete at water saturated state, compressive strength, splitting tensile strength, and static modulus of elasticity.

Density of the concrete has been examined on cubical specimens with 150 mm edge length, according to standard EN 12390-7 [17]. Mass of the specimens has been measured by electronic scale "KERN" with accuracy class of 0.1 g.

Compression strength has also been tested on cubical specimens with 150 mm edge, according to standard EN 12390-3 [18], using digital hydraulic press "UTEST UTC-5740" with accuracy class of 0.5% (Fig. 1(a)). The splitting tensile strength has been tested according to standard EN 12390-6 [19] on cylindrical specimens with diameter of 150 mm and height 300 mm, using digital hydraulic press "UTEST UTC-5600" with accuracy class of 0.5%. Fig. 1(b) presents view of the testing device and the specimen during the test. Examination of the static modulus of elasticity has been also conducted on cylindrical specimens with diameter of 150 mm and height 300 mm according to standard EN 12390-13 [20], using digital hydraulic press "UTEST UTC-5740" and three digital extensometers "CONTROLS 55-C0222/F". This examination is presented in Fig. 1(c).

Mean values out of three results of examined characteristics, as well as standard deviations, are presented in Table 1.

All material tests have been completed in the Laboratory for building materials at the Faculty of Civil Engineering and Architecture, University of Niš, Serbia.

2.2 Experimental testing of impact strength of a concrete slab

The impact strength of the concrete slabs has been conducted using the Drop-weight test method, in the same laboratory as the material tests. The test has been done on a concrete slab with dimensions 400 × 400 × 50 mm (Fig. 2(a)). A cylindrical steel weight with mass of 3.00 kg (Fig. 2(b)) has been dropped from height of 0.30 m. The concrete specimen was fixed into the test frame, and the weight was guided by a vertical tube, so the impacts were concentrated in the middle of the top slab surface. The test setup is shown in Fig. 2(c).

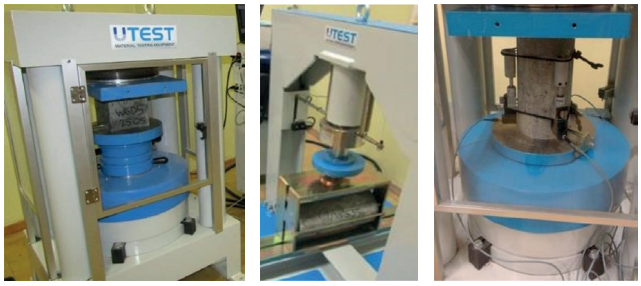

(a) (b) (c)

Fig. 1 Examination of hardened concrete characteristics: (a) compression strength; (b) splitting tensile strength; (c) static modulus of elasticity

Table 1 Basic material characteristics of the hardened concrete

Characteristic	Mean value	Standard deviation	Unit
Density of the hardened concrete	2347	10.24	kg/m^3
Compressive strength f_c	59.78	0.95	MPa
Splitting tensile strength f_{ct}	4.23	0.13	MPa
Static modulus of elasticity E_c	36.50	0.16	GPa

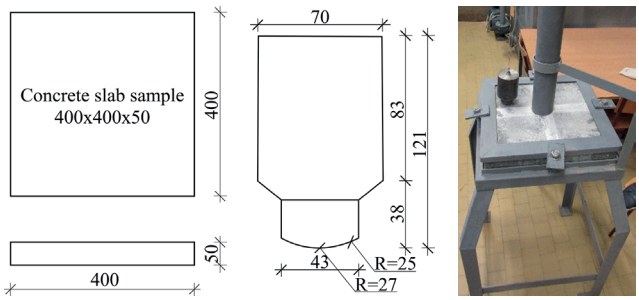

(a) (b) (c)

Fig. 2 Experimental test (measures in mm); (a) slab specimen; (b) steel weight; (c) test setup with specimen

The weight was dropped in equal time intervals, and occurrence of cracks in concrete has been tracked at the top and bottom surface of the slab. Fracture of the specimen has been defined by occurring of the cracks both at the bottom and the top side of the slab, which meant that the cracks have propagated throughout the total depth of the specimen.

Based on the number of impacts and the drop height, one may calculate the impact energy at the fracture of the specimen, as $E = N \times m \times g \times h$ [21], where E denotes impact energy [J], N denotes number of impacts, m denotes drop-weight mass [kg], g denotes gravity acceleration of 9.81 m/s^2 and h denotes drop height of the drop-weight [m].

The results of the Drop-weight test for all three specimens are given in Table 2. During the test, the first crack occurred at the bottom surface of the slab, and it happened after 13 impacts, which represented the mean value. After that, cracks propagated further through the depth of the slab. Occurrence of the cracks on the top surface of the slab implied that the cracks propagated throughout the total depth of the slab, and fracture criterion has been achieved after 16 impacts, again, a mean value from three tests. Typical examples of the occurrence of the first crack and of the specimen fracture are given in Fig. 3.

The presented experimental setup and result data have been used for calibrating and validating the numerical model presented in the following sections.

3 Numerical modelling using finite element method

In this research, two numerical models for determining the impact strength of the concrete slab have been proposed, using the FEM and appropriate software. The established procedure for reliable modelling of a drop-weight test of concrete slab is presented in this section in detail. The models have been validated using experimental results. The main parameter for validation was the number of impacts

Table 2 Drop-weight test results

Specimen	No. of impacts for the 1st crack	Impact energy at the 1st crack [J]	No. of impacts for fracture	Impact energy at the fracture [J]
1	13	114.74	16	141.26
2	13	114.74	15	132.44
3	14	123.57	16	141.26

(a) (b)

Fig. 3 Characteristic examples from the drop-weight test: (a) occurrence of the first crack; (b) specimen fracture

required for specimen fracture. The proposed numerical models can be used in further research of the impact strength of concrete slab instead of costly experiments. One must bear in mind that for every new analysis of this type, input data regarding physical and mechanical characteristics of the concrete material have to be determined.

Numerical modelling of the drop-weight tests falls into high demanding tasks in the FEM field. The problem includes dynamic aspects and highly non-linear behavior of the specimen, like plastic deformations and contact phenomena. The duration of the impact is very short, with value order of approx. 0.1 ms. That was the reason for selection of the Explicit dynamic analysis in this research.

Considering this, and the selected Explicit dynamic analysis, appropriate material models for concrete should have been chosen, as well as the software that supports it. For this research, two sophisticated software have been selected, ABAQUS/Explicit and ANSYS Workbench, as capable for this research task.

3.1 Modelling concepts

Explicit dynamics analysis is capable to reveal the dynamic response of structures exposed to short-time impact loads. In order to obtain a stable analysis progression, the time increment has to be set as proportional to the smallest finite element dimension in the model, and inversely proportional to the sound speed in the material used [22, 23]. As a result, the time increments can last a few microseconds, and the complete analysis may have several thousand-time steps, or analysis cycles [22, 23].

Geometry of the FE numerical models of the concrete slab and the drop-weight has been created according to the geometry of the test specimen and the weight used (Fig. 2). For the initial position in the numerical analysis, the moment of the contact between the drop-weight and the concrete slab has been chosen. Model geometry created in the software package ABAQUS/Explicit is shown in Fig. 4, and the geometry of the model in the software package Ansys Workbench is the same.

In the experimental setup, the concrete slab was supported along all edges of its bottom surface. In line with that, in the FE model all translational degrees of freedom were constrained on these edges. The drop-weight was restrained along the top base with prevented translations in X- and Z-direction, enabling only vertical move (Fig. 4).

The steel material model of the drop-weight has been taken as linear elastic, since no significant deformation of the weight body was expected, and the weight itself was not the subject of the analysis. The steel material has been defined by its modulus of elasticity E = 210 GPa, Poisson's ratio ν = 0.3, and the mass density γ = 7850 kg/m^3. Mass density of concrete was 2347 kg/m^3, (Table 1).

3.2 Explicit dynamics FE analysis using the concrete damage plasticity (CDP) model

3.2.1 Material model

The CDP material model, implemented in the ABAQUS/Explicit software, has been used in this research. For this analysis, the characteristics of the concrete material are defined based on mechanical characteristics and recommendations from [24], using the following relations:

$$\sigma_c = \frac{k\eta - \eta^2}{1+(k-2)\eta} f_c;\ \eta = \frac{\varepsilon_c}{\varepsilon_{c1}};\ k = 1.05E_c\frac{\varepsilon_{c1}}{f_c}, \quad (1)$$

where:

ε_c is compression strain and it is used as argument for determining compression stress σ_c,

ε_{cl} = 0.00245 is the strain at the maximal stress,

ε_{cul} = 0.00350 is the ultimate strain,

f_c is compressive strength,

E_c is modulus of elasticity.

The stress-strain diagram of the concrete at compression is presented in Fig. 5(a). Stress-strain diagram of the concrete under tension is defined using the relation given in [25]:

$$\sigma_t = f_t\left(\frac{\varepsilon_{cr}}{\varepsilon_t}\right)^{0.40}, \quad (2)$$

where:

ε_t is tension strain and it is used as argument for determining tension stress σ_t,

f_t is tensile strength of concrete,

ε_{cr} is strain at the tensile strength of concrete.

Tensile strength of concrete cannot be easily determined by experiment. Therefore, it is defined based on the experimentally obtained splitting tensile strength (f_{ct}), and according to the relation defined in [24], as $f_t = 0.90 f_{ct}$.

With such adopted material model, the tensile strength of concrete is f_t = 3.807 MPa, and correspondent strain is ε_{cr} = 0.000104 calculated from the Hooke's law ($\varepsilon_{cr} = f_t/E_c$). Stress-strain diagram of concrete at tension is presented in Fig. 5(b).

Since this research implies exposure of concrete specimen to a series of impacts up to its fracture, it may be expected that concrete will endure significant plastic deformations. Therefore, an appropriate material model that describes the

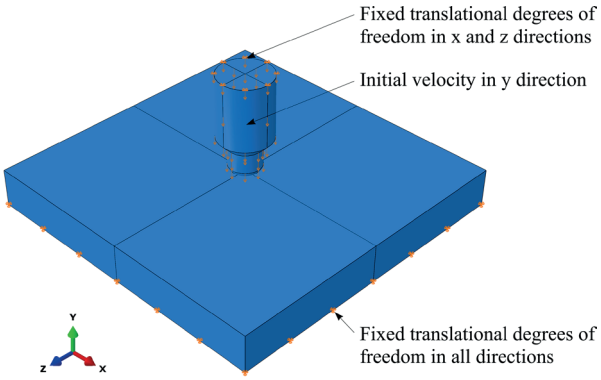

Fig. 4 FE model geometry and boundary conditions

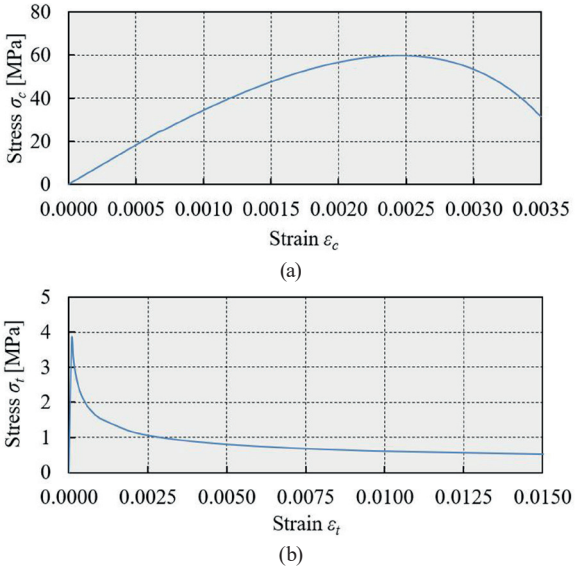

Fig. 5 Stress-strain diagram for concrete: (a) compression; (b) tension

plastic behavior of the concrete should have been applied. The adopted CDP model introduces damage of the concrete both due to compression and tension, and has its ground in Fracture mechanics, i.e., on the Drucker-Prager's hyperbolic function of flow of the plastic potential. Taking into account [23], this model has been selected as adequate for modelling quasi-brittle materials, see also [26, 27]. Prior to applying the CDP material model in analysis, several input parameters need to be defined, as described below.

Dilatation angle (dilatancy) ψ has been adopted as $\psi = 30°$, according to [27]. For the eccentricity of the plastic potential ϵ, and for the relation between the biaxial and uniaxial yield stress under compression σ_{b0}/σ_{c0}, default values have been chosen, i.e., $\epsilon = 0.1$ and $\sigma_{b0}/\sigma_{c0} = 1.16$, as recommended in [26]. Also, default value has been adopted for the relation of the magnitude of the deviatoric stress under tension and compression, $K = 0.666$ [27]. Finally, the nondimensional viscosity parameter μ, has been taken as $\mu = 0.000001$. Namely, behavior of the concrete is very complex, and may cause convergence issues. This is always the case when the used material model encompasses softening phenomena. In the software used here this class of problem is overcome by the so-called viscoplastic regularization of the constitutive equations. That way, using a very small value for the viscosity parameter μ may help the convergence of the model in the softening range, without affecting the reliability of the results [23].

When concrete material is unloaded after reaching the strain softening branch of the stress-strain curves (both for compression and tension), the unloading branch become weakened. This means that the elastic stiffness of the material becomes degraded by damage. In the CDP model this degradation is achieved by reducing the initial modulus of elasticity multiplying it by factor $1–d_c$ for compression, and by factor $1–d_t$ for tension (Fig. 6) [23, 28]. Damage parameters for compression d_c, and for tension d_t [23], are determined by the following relations:

$$d_c = 1 - \frac{\sigma_c}{f_c};\ d_t = 1 - \frac{\sigma_t}{f_t}. \tag{3}$$

Fig. 7 presents dependences of the mentioned damage parameters on concrete strains for the analyzed model. It should be remarked that values for compression used in the software were defined with respect to the inelastic strains ε_c^{in}, and values for tension were defined with respect to the cracking strains ε_t^{cr}. Inelastic strain in compression, and cracking strain in tension, represents total strain minus

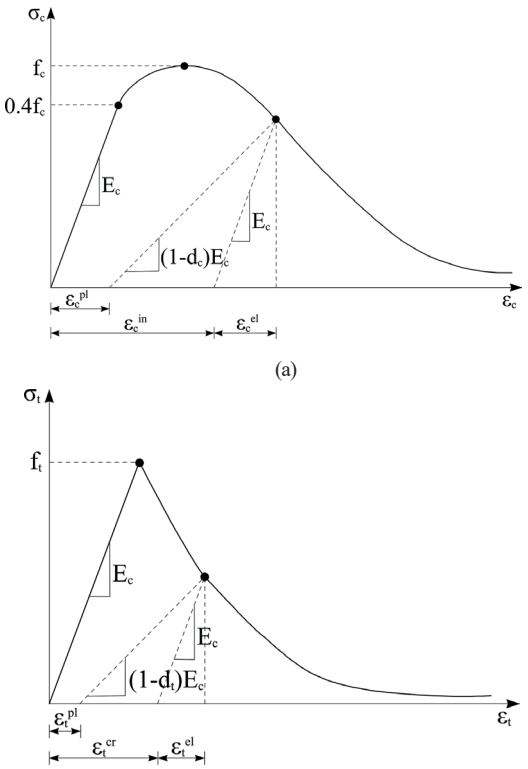

Fig. 6 Material damage model: (a) compression; (b) tension

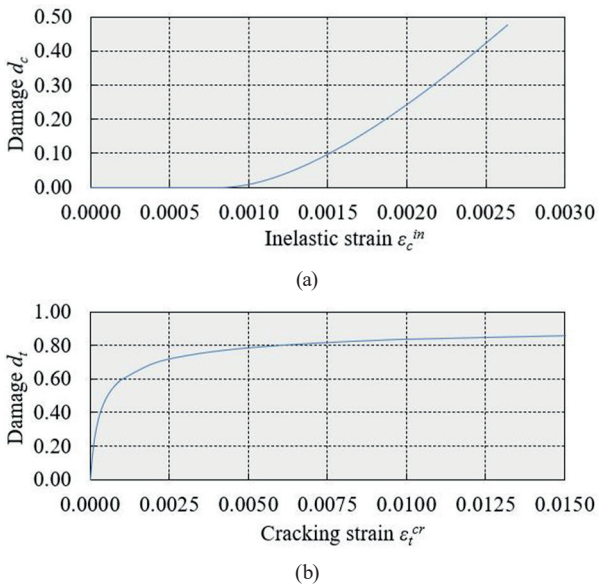

Fig. 7 Damage parameters in the CDP model: (a) compression; (b) tension

elastic strain corresponding to the undamaged material. Whereat the threshold of the elastic behavior of the analyzed concrete under compression was $0.4\,f_c = 22.91$ MPa (with correspondent strain of 0.000655), and under tension $f_t = 3.807$ MPa (with correspondent strain of 0.000104).

Based on the data of the inelastic strain ε_c^{in} and damage parameter d_c in compression, and cracking strain ε_t^{cr} and damage parameter d_t in tension, the plastic strain in compression ε_c^{pl} and plastic strain in tension ε_t^{pl} are calculated by software [23] as follows:

$$\varepsilon_c^{pl} = \varepsilon_c^{in} - \frac{d_c}{1-d_c}\frac{\sigma_c}{E_c};\ \varepsilon_t^{pl} = \varepsilon_t^{cr} - \frac{d_t}{1-d_t}\frac{\sigma_t}{E_c}. \quad (4)$$

3.2.2 Finite element mesh

The slab and the drop-weight were meshed with solid FE. Here it must be noted that, in a case of dominant bending deformation and use of solid FE with linear shape functions, a large shear stiffness can occur, which is not realistic. This phenomenon, known as "shear locking", was prevented using hexahedral finite elements with linear shape functions and reduced integration for stiffness matrix determination (denoted in the software as C3D8R) [23]. Global edge size of the FE was 5 mm, resulting with 68608 elements and 77489 nodes. In the narrow zone of contact of the drop-weight and the slab, mesh size was 2 mm, in order to cover the expected stress concentration. The finite element mesh of the model is shown in Fig. 8.

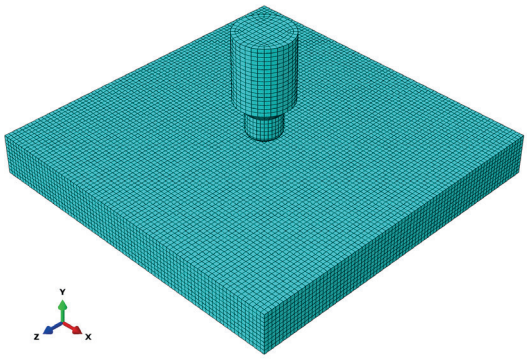

Fig. 8 Finite element mesh

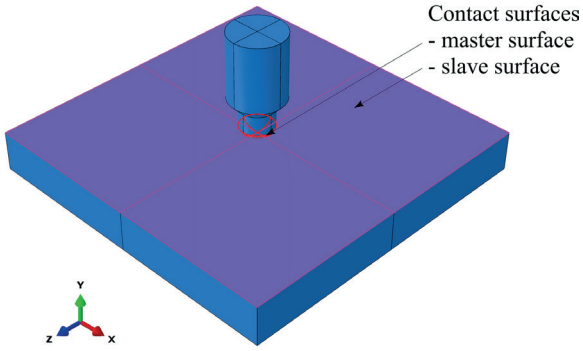

Fig. 9 Contact surfaces

3.2.3 Analysis parameters

For the drop-weight simulation, an initial velocity has been applied to the drop-weight, and it has been calculated based on the travelling time of the weight dropped from the height of 0.300 m (taken from the experimental data) with respect to the slab top surface, as $v = (2gh)^{0.5} = 2.4261$ m/s, where h denotes the drop height [m], g denotes the gravity acceleration [m/s^2] and v denotes the drop weight velocity [m/s].

Interaction between the drop-weight and the concrete slab has been modelled with a standard surface-to-surface contact (Fig. 9). The interaction has been defined in such a way to transfer normal pressure without friction between contact bodies.

Setting the appropriate procedure of analysis in such complex problem is of utmost importance. In this research, the following strategy has been applied:

- every impact of the drop-weight onto the slab was analyzed through a single load step,
- one completed load step was followed by unloading,
- next impact has been applied after completing the previous one, using the restart command.

For every impact, lasting of the contact of the two bodies, the drop-weight and the slab, was set as 0.0001 s, according to recommendations in the literature related to impact analysis using Explicit dynamics [22, 29].

3.2.4 Analysis results and discussion

As it has been defined in the experimental part of the research, it was adopted that fracture of the specimen arose when the cracks propagated throughout the total depth of the slab, and it was related to the corresponding number of impacts. Since the CDP model does not support the development of cracks, the crack occurrence was defined implicitly. In other research it is recommended to adopt that cracks open at strains several dozen times greater than the strain at tension strength [30]. In this research, the model calibration showed that satisfying results were obtained if the cracks opened at strain 50 times greater than the strain at tension strength, whereat the damage parameter d_t took value of 0.80. During this analysis, the number of impacts needed for developing of the cracks has also been tracked. Unlike the experimental test, here it was possible to follow the crack development implicitly through the vertical midplane section of the slab.

Fig. 10(a) presents appearance of the crack field at the bottom surface of the slab after $N = 11$ impacts, when first cracks occurred.

Fig. 10(b) presents crack propagation through the slab depth in the vertical midplane after $N = 14$ impacts. It is marked by red and orange contours in the damage parameter legend, indicating the values higher than 0.80,

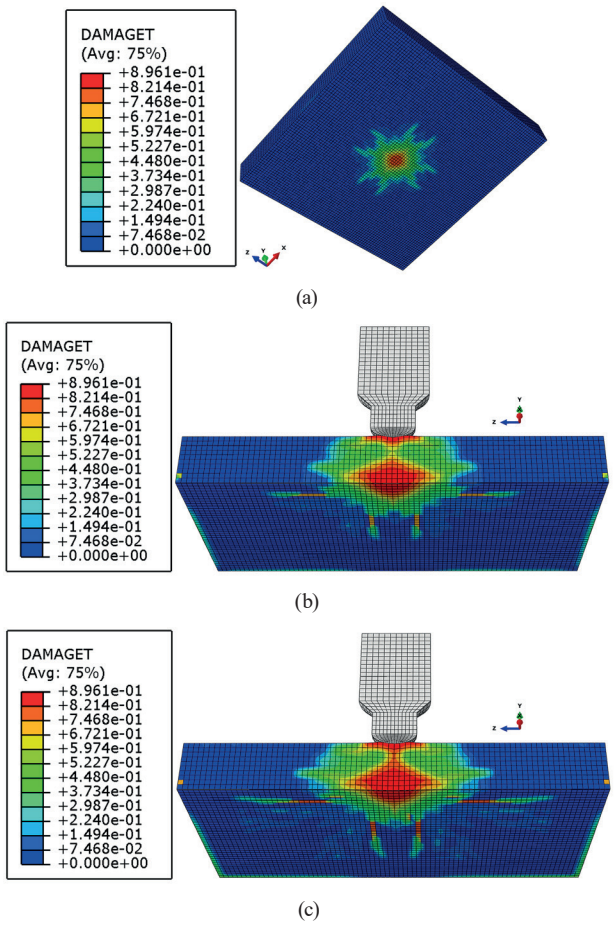

Fig. 10 Damage parameter in tension: (a) impact no. 11, occurrence of the first cracks; (b) impact no. 14, crack propagation; (c) impact no. 17, fracture

as described above. One may see that the cracks developed rather abruptly, and they could be noticed at the bottom surface, as well as at the top surface, under the drop-weight. The crack field narrows towards the top third of the slab, where cracks still do not occur.

Fig. 10(c) presents contours of the cracks after $N = 17$ impacts. The crack field from the top of the slab is now joined with the crack field from the bottom, via a narrow "neck" represented by orange contours. That way, the crack field becomes continuous, signaling fracture.

Comparison between the crack fields from the experimental testing (Fig. 3) and from the numerical FE analysis (Fig. 10) does not show high degree of congruence, especially regarding the symmetry of the cracks. However, observing the experimental crack patterns, one may see that they all meet in the center of the slab, very similar to the crack pattern from the numerical analysis.

The obtained results show good agreement with the experimental test, with small deviation (Table 3). Observing the comparative results, one may note that the numerical analysis here is over-conservative regarding the occurrence of the first cracks, but under-conservative regarding the arising of fracture. Nevertheless, the prediction of fracture does not deviate significantly, only 5.88%, while the prediction of the first crack occurrence shows somewhat lower accuracy, deviating 18.18%.

Table 3 Experimental vs. numerical results (CDP material model)

Method	No. of impacts for the 1st crack	No. of impacts for fracture
Experimental test	13	16
Numerical test	11	17
Deviation [%]	18.18	-5.88

3.3 Explicit dynamics FE analysis using Riedel-Hiermaier-Thoma model (RHT)

3.3.1 Material model

For this analysis, the RHT concrete model and ANSYS Workbench Explicit dynamics module has been used to model the concrete slab. This is an advanced plasticity model used for brittle materials [31–33].

This constitutive model is a combined plasticity and shear damage model, and it is particularly useful for modeling concrete in a case of dynamic loading. The model is formulated in such way that complete input data can be scaled using the nominal compressional strength of concrete [22]. In this research, the compressional strength of the slab concrete was f_c = 59.78 MPa, and the tension strength was defined using the ratio of the tensile and compression strength f_t / f_c = 3.807 / 59.78 = 0.06368.

The remained input data for this model have been taken as default values given in the software [22] (Table 4).

3.3.2 Finite element mesh

The complete FE model was meshed with solid finite elements. For the slab, hexahedral FE shapes with 8 nodes and 3 translational degrees of freedom (DOF) were used, due to the regularity of the slab shape. The drop-weight, having more complex shape, was meshed with tetrahedrons, prisms, and pyramids. The overall edge size of the mesh was 5 mm, which resulted with 72312 elements and 79296 nodes. In the narrow zone of contact of the drop-weight and the slab, mesh size was 2 mm, in order to cover the expected stress concentration and to compensate the low order of the finite elements of the drop-weight. The FE mesh of the model is shown in Fig. 11.

Table 4 Input data for RHT concrete model

Name	Value
Compressive Strength (f_c) [MPa]	59.78
Tensile Strength (f_t / f_c)	0.06368
Shear Strength (f_s / f_c)	0.18
Intact failure surface constant A (A_{FAIL})	1.6
Intact failure surface exponent N (N_{FAIL})	0.61
Tens. / Comp. Meridian ratio ($Q_{2.0}$)	0.6805
Brittle to Ductile Transition (BQ)	0.0105
Hardening Slope	2
Elastic Strength / f_t	0.7
Elastic Strength / f_c	0.53
Fracture Strength Constant (B)	1.6
Fracture Strength Exponent (m)	0.61
Compressive strain rate exponent (α)	0.032
Tensile strain rate exponent (δ)	0.036
Maximum fracture strength ratio ($SFMAX$)	1E+20
Use cap on elastic surface	Yes
Damage constant $D1$	0.04
Damage constant $D2$	1
Minimum strain to failure	0.01
Residual Shear modulus fraction	0.13

3.3.3 Analysis parameters

According to the given drop height, the initial velocity of the drop-weight at the impact moment has been calculated by the applied software. For this particular numerical analysis, a series of impacts in the experiment was replaced by a single impact. Based on this, and assuming equality of the total kinetic energy produced by series of impacts in the experiment and the total kinetic energy generated by one impact in the FE analysis, the drop height after N impacts was defined as $H_{calc} = Nh$.

The impact duration between the concrete slab and the drop-weight during one impact has been assumed as 0.0001 s, so the total analysis time for analysis of the influence of the N impacts has been defined as $t = 0.0001\ N$.

Interaction between the drop-weight and the concrete slab has been modelled with a frictionless surface-to-surface contact, similar to the previously defined contact analysis (Section 3.2.3, Fig. 9), which transfers forces normal to the contact surfaces allowing separation after contact [22].

3.3.4 Analysis results and discussion

As seen in the Section 2.2 and Section 3.2.4, fracture of the slab arises when cracks propagate throughout the total depth of the slab, and it is accompanied with certain

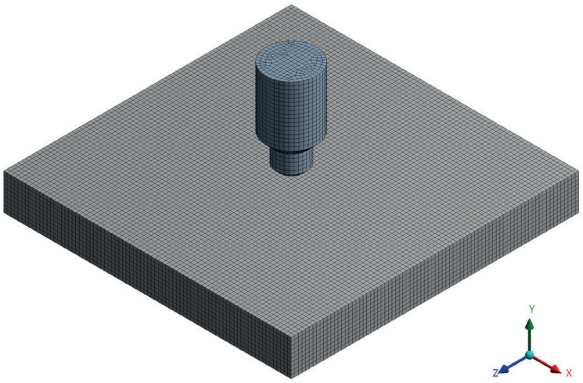

Fig. 11 Finite element mesh

number of impacts. Like the CDP model, the RHT concrete model does not support the development of cracks, so the crack occurrence has been defined implicitly, using the damage parameter. In the software used [22], this parameter ranges from 0 to 1, where 0 stands for intact material, and 1 stands for fully fractured material. For this particular analysis, the value of the damage parameter higher than 0.80 has been adopted as crack occurrence threshold, analogously with the previous analysis (see Section 3.2.4).

Development of the cracks has been tracked here implicitly as well, observing the bottom of the slab and its vertical midplane.

Fig. 12(a) presents the crack field at the bottom of the slab after $N = 13$ impacts, when the first cracks occurred. The pattern is highly symmetrical, with slab diagonals as symmetry axes. The cracks are represented by red and orange contours, which denote damage parameter values that exceed value of $0.77778 \approx 0.80$. They are spread around the center of the slab where the drop-weight impact is striking, as expected. Besides that, cracks can be visible near the bottom apexes of the slab. They are consequence of the boundary conditions and sharp change of the slab contour at the apexes. The lower-value contours (green to cyan), with values under 0.66667 spread diagonally and indicate further propagation of the cracks along the bottom slab surface.

Fig. 12(b) is the contour presentation of the cracks after $N = 14$ impacts. In the vertical midplane section damaged elements protrude to the bottom of the slab, thus showing the crack propagation throughout the slab depth. The form of the damaged elements, i.e., of the cracks, is in the shape of a truncated pyramid, much alike to the problem of fracture of concrete foundation column footings by punching shear. These results confirm the results of other investigations [34]. Like in the analysis given in Section 3.2, the continuous crack field denotes fracture of the slab. Here, the cracks have been developed even more abruptly than

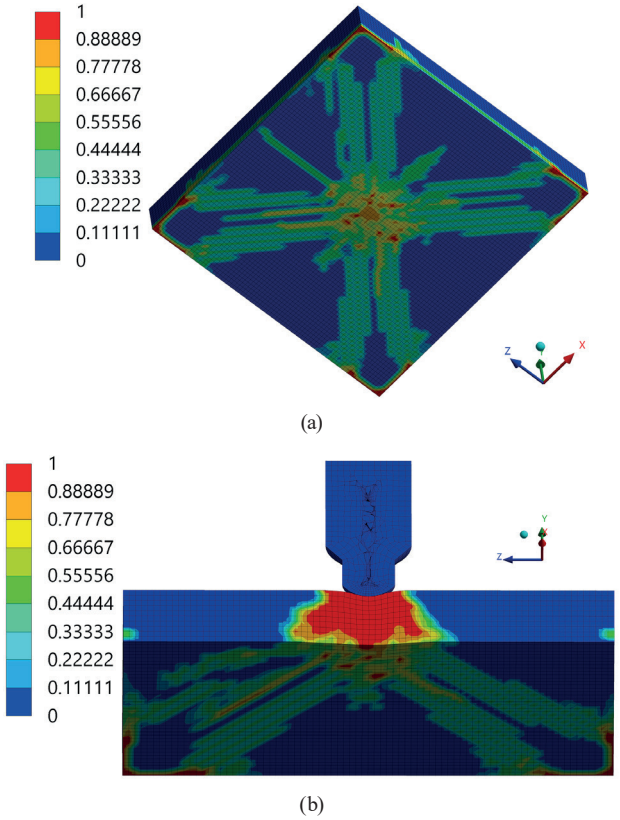

Fig. 12 Damage parameter: (a) impact no. 13, occurrence of first cracks; (b) impact no. 14, occurrence of fracture

in the previous analysis. Namely, the number of impacts needed for the first cracks and the number needed for the slab fracture differ by just 1, i.e., they are consecutive.

The obtained results showed very good agreement with the experimental test, with minimal deviation (Table 5). The numerical analysis showed 100% agreement regarding occurrence of the first cracks, and for the arising of fracture, it was conservative, thus being on the safe side.

4 Conclusions

The Explicit dynamics analysis has been chosen in this research as recommended both by researchers and by software guides. In accordance with the type of analysis and the software applied, two existing material models for concrete have been used: the Concrete damage plasticity model – CDP (implemented in ABAQUS/Explicit software), and the Riedel-Hiermaier-Thoma model – RHT (implemented in ANSYS Workbench software). The problem has been analyzed by both available software and applying correspondent material models, with validating the analysis parameters using the experimental data. From the conducted investigation, the following conclusions can be drawn:

Table 5 Experimental vs. numerical results (RHT material model)

Method	No. of impacts for the 1st crack	No. of impacts for fracture
Experimental test	13	16
Numerical test	13	14
Deviation [%]	0.0	14.3

1. The proposed numerical FE models can be successfully used in research of low velocity impact problem, and serve as a complement to the experimental drop-weight tests for determining the impact strength of concrete.

2. Conducted FE analyses show that solving impact problems is very complex and includes nonlinearities like plasticization and contact phenomena, cracking, and fracture. Because of that, solution of this class of problem demands careful selection of the material model that will be used for concrete, as well as the type of FE analysis. Both aspects are interrelated, and require software support.

3. Results of both selected analyses and applied material models showed good agreement with the experimental testing. It is especially related to the quantitative aspect of the analysis, i.e., of the number of impacts required for crack initiating and for the specimen fracture.

4. The CDP model appeared to be demanding regarding the preparatory calculations needed as input data for analysis. The obtained results for impact strength showed certain deviation compared to the experimental ones. Namely, in case of the occurrence of the first crack the deviation was 18.18 %, but the number of impacts required for fracture, as the most significant value, deviated only 5.88%.

5. The RHT model is quite simple to apply, requiring minimal input data. Only the compression strength and relation between the compression and tension strength is needed, and those values have been taken from the experimental testing of the concrete material. The remained data are taken as default values provided by the software used. The results showed very good agreement with the experimental tests, with absolute agreement regarding the number of impacts needed for occurrence of the first cracks, and the deviation of 14.3% for the number of impacts needed for fracture.

6. The crack patterns, here represented by the so-called "damage parameter", showed less matching with the experimental tests. The explanation for this lies in the fact that during the experiment, the cracks appear in quite stochastic manner, thus stressing out the nature of the fracture under impact. However, the average of several

experimental crack patterns in some sense is expected to be similar to the crack patterns found in the finite element results. The propagation of the cracks, represented by damaged finite elements, throughout the depth of the slab showed that the fracture mechanism in the FE analyses has been described well. It especially stands for the model built using the RHT material model. It must be also remarked that the insight into the cross-section crack propagation could be tracked during the FE analysis, unlike the experiment.

7. The proposed numerical FE models offer reliable tool for predicting the development of the cracks and fracture of concrete slabs under impact load, and they can significantly support the experimental work.

Further research should by all means include analysis of concrete specimens with various dimensions and support conditions, and application on reinforced slabs. Also, the phenomenon of low agreement of the crack patterns obtained by the FE analysis and the experimental testing should be addressed in more detailed manner in further research. High velocity impact strength of concrete slabs, as a special class of Explicit dynamics, could also be a subject of further analysis.

Acknowledgement

The study was supported by Ministry of Education, Science and Technological Development of the Republic of Serbia (grant no. TR 36028, TR 36016 and TR 36017).

References

[1] ACI Committee 544 "ACI 544.2R-89 Report, Measurement of Properties of Fiber Reinforced Concrete", American Concrete Institute, Detroit, MI, USA, 1999.

[2] Zakić, D. "Istraživanje parametara duktilnosti i udarne otpornosti sitnoznih betona mikroarmiranih sintetičkim vlaknima" (Investigation of parameters of ductility and impact resistance of fine-grained concrete micro-reinforced with synthetic fibers), PhD Thesis, University of Belgrade, 2010.

[3] Saatci, S., Vecchio, F. J. "Effects of Shear Mechanisms on Impact Behavior of Reinforced Concrete Beams", ACI Structural Journal, 106(1), pp. 78–86, 2009. https://doi.org/10.14359/56286

[4] Yılmaz, M. C., Anıl, Ö., Alyavuz, B., Kantar, E. "Load displacement behavior of concrete beam under monotonic static and low velocity impact load", International Journal of Civil Engineering, 12(4), pp. 488–503, 2014. [online] Available at: http://www.iust.ac.ir/ijce/article-1-917-en.html&sw= [Accessed: 26 June 2022]

[5] Andersson, A. "Impact loading on concrete slabs - Experimental tests and numerical simulations", Royal Institute of Technology (KTH), Department of Civil and Architectural Engineering, Division of Structural Engineering and Bridges, Stockholm, Sweden, TRITA-BKN Report 153, 2014.

[6] Zaini, S. S. "Impact Resistance of Pre-Damaged Ultra-High Performance Fibre Reinforced Concrete (UHPFRC) Slabs", PhD Thesis, University of Liverpool, 2015.

[7] Wang, Y., Liu, J., Xiao, Z., Zhao, F., Cheng, Y. "Experiment and Simulation Study on the Dynamic Response of RC Slab under Impact Loading", Shock and Vibration, 2021, 7127793, 2021. https://doi.org/10.1155/2021/7127793

[8] Tuğrul Erdem, R., Gücüyen, E. "Non-linear analysis of reinforced concrete slabs under impact effect", Građevinar, 69(6), pp. 479–487, 2017. https://doi.org/10.14256/JCE.1557.2016

[9] Senthil, K., Kubba, Z., Sharma, R., Thakur, A. "Experimental and Numerical Investigation on Reinforced Concrete Slab under Low Velocity Impact Loading", In: IOP Conference Series: Materials Science and Engineering, 1090, 012090, 2020. https://doi.org/10.1088/1757-899X/1090/1/012090

[10] Yılmaz, T., Kıraç, N., Anıl, Ö., Tuğrul Erdem, R., Kaçaran, G. "Experimental Investigation of Impact Behaviour of RC Slab with Different Reinforcement Ratios", KSCE Journal of Civil Engineering, 24(1), pp. 241–254, 2020. https://doi.org/10.1007/s12205-020-1168-x

[11] Laczák, L. E., Károlyi, G. "Local Effects of Impact into Concrete Structure", Periodica Polytechnica Civil Engineering, 60(4), pp. 573–582, 2016. https://doi.org/10.3311/PPci.8605

[12] Al Rawi, Y., Temsah, Y., Baalbaki, O., Jahami, A., Darwiche, M. "Experimental Investigation on the Effect of Impact Loading on Behavior of Post-Tensioned Concrete Slabs", Journal of Building Engineering, 31, 101207, 2020. https://doi.org/10.1016/j.jobe.2020.101207

[13] Sadraie, H., Khaloo, A., Soltani, H. "Dynamic performance of concrete slabs reinforced with steel and GFRP bars under impact loading", Engineering Structures, 191, pp. 62–81, 2019. https://doi.org/10.1016/j.engstruct.2019.04.038

[14] Kheyroddin, A., Arshadi, H., Khedri, J. "The Resistance of Fiber-reinforced Concrete with Steel Fibers and CFRP to Drop-weight Impact", Periodica Polytechnica Civil Engineering, 65(2), pp. 666–676, 2021. https://doi.org/10.3311/PPci.17477

[15] Yılmaz, T., Anil, Ö., Tuğrul Erdem, R. "Experimental and numerical investigation of impact behavior of RC slab with different opening size and layout", Structures, 35, pp. 818-832, 2022. https://doi.org/10.1016/j.istruc.2021.11.057

[16] CEN "EN 12390-2 - Testing hardened concrete - Part 2: Making and curing specimens for strength tests", European Committee for Standardization, Brussels, Belgium, 2019.

[17] CEN "EN 12390-7 - Testing hardened concrete - Part 7: Density of hardened concrete", European Committee for Standardization, Brussels, Belgium, 2019.

[18] CEN "EN 12390-3 - Testing hardened concrete - Part 3: Compressive strength of test specimens", European Committee for Standardization, Brussels, Belgium, 2019.

[19] CEN "EN 12390-6 - Testing Hardened Concrete - Part 6: Tensile Splitting Strength of Test Specimens", European Committee for Standardization, Brussels, Belgium, 2009.

[20] CEN "EN 12390-13 - Testing hardened concrete - Part 13: Determination of secant modulus of elasticity in compression", European Committee for Standardization, Brussels, Belgium, 2013.

[21] Daneshvar, K., Moradi, M. J., Khaleghi, M., Rezaei, M., Farhangi, V., Hajiloo, H. "Effects of impact loads on heated-and-cooled reinforced concrete slabs", Journal of Building Engineering, 61, 105328, 2022.
https://doi.org/10.1016/j.jobe.2022.105328

[22] ANSYS, Inc. "Ansys Explicit Dynamics Analysis Guide" [online] Available at: http://www.ansys.com

[23] Dassault Systems "Abaqus Theory Manual" [online] Available at: http://130.149.89.49:2080/v6.14/books/stm/default.htm

[24] CEN "EN 1992:2004 Design of concrete structures - Part 1-1: General rules and rules for buildings", European Committee for Standardization, Brussels, Belgium, 2004.

[25] Wang, T., Hsu, T. T. C. "Nonlinear finite element analysis of concrete structures using new constitutive models", Computers and Structures, 79, pp. 2781–2791, 2001.
https://doi.org/10.1016/S0045-7949(01)00157-2

[26] Alfarah, B., López-Almansa, F., Oller, S. "New methodology for calculating damage variables evolution in Plastic Damage Model for RC structures", Engineering Structures, 132, pp. 70–86, 2017.
https://doi.org/10.1016/j.engstruct.2016.11.022

[27] Petrović, Ž., Milošević, B., Zorić, A., Ranković, S., Mladenović, B., Zlatkov, D. "Flexural Behavior of Continuous Beams Made of Self-Compacting Concrete (SCC) – Experimental and Numerical Analysis", Applied Sciences, 10(23), 8654, 2020.
https://doi.org/10.3390/app10238654

[28] Lubliner, J., Oliver, J., Oller, S., Oñate, E. "A plastic-damage model for concrete", International Journal of Solids and Structures, 25(3), pp. 299–326, 1989.
https://doi.org/10.1016/0020-7683(89)90050-4

[29] Lee, H.-H. "Finite Element Simulations with ANSYS WORKBENCH 16, Theory, Applications, Case Studies", SDC Publications, 2015. ISBN-13: 978-1-58503-983-8

[30] Shamass, R., Zhou, X., Aldano, G. "Finite-Element Analysis of Shear-Off Failure of Keyed Dry Joints in Precast Concrete Segmental Bridge", Journal of Bridge Engineering, 20(6), 04014084, 2015.
https://doi.org/10.1061/(ASCE)BE.1943-5592.0000669

[31] Riedel, W., Thoma, K., Hiermaier, S., Schmolinske, E. "Penetration of Reinforced Concrete by BETA-B-500, Numerical Analysis using a New Macroscopic Concrete Model for Hydrocodes", In: Proceedings of the 9. International Symposium on Interaction of the Effects of Munitions with Structures, Strausberg, Berlin, 1999, pp. 315–322.

[32] Riedel, W. "Beton unter dynamischen Lasten: Meso- und makromechanische Modelle und ihre Parameter" (Concrete under dynamic loads: meso- and macro-mechanical models and their parameters), Fraunhofer IRB Verlag, 2004. ISBN 3-8167-6340-5

[33] Riedel, W., Kawai, N., Kondo, K. "Numerical Assessment for Impact Strength Measurements in Concrete Materials", International Journal of Impact Engineering, 36, pp. 283–293, 2009.
https://doi.org/10.1016/j.ijimpeng.2007.12.012

[34] Vacev, T., Bonić, Z., Prolovićc, V., Davidović, N., Lukić, D. "Testing and finite element analysis of reinforced concrete column footings by punching shear", Engineering Structures, 92, pp. 1–14, 2015.
https://doi.org/10.1016/j.engstruct.2015.02.027